*Green Sciences, 27, **3**, 24—32, 10.2478/pjct-2025-0014*

Bridge crack self-repairing based on nanosilica-modified bacterial solution

Yejun Zhou[1], Shengli Zhang[2*], Xiujuan Liu[3], Jun Yang[3]

[1]Jiangxi Transportation Institute Co., Ltd., Nanchang, Jiangxi, China
[2]Liuzhou Institute of Technology, Liuzhou, Guangxi, China
[3]Sichuan Central Inspection Technology Inc., Zigong, Sichuan, China
[*]*Corresponding authors:* e-mail: Zhang5Shenglili@163.com

To address the challenge of self-healing concrete cracks (CCs) in bridge structures, a nano-SiO_2-modified bacterial solution was developed and systematically evaluated for its effectiveness in enhancing crack healing performance. Calcium lactate, used as a calcium source, increased the surface roughness of calcium carbonate crystals, enhancing Ca^{2+} adsorption and achieving a mineralization efficiency (ME) of 2.18 mol/h at 36 h. The optimized application process—three treatments at 15-minute intervals—significantly reduced the concrete's chloride migration coefficient (8.48×10^{-13} m^2/s), electrical flux (327 C), and carbonation depth (2.8 mm after 13 days). After 28 days, the bacterial group repaired over 95% of both primary and secondary crack areas. These improvements are attributed to nano-SiO_2 providing a high specific surface area for microbial adhesion and promoting calcium carbonate precipitation, thus accelerating crack closure. The proposed nano-SiO_2-modified bacterial solution offers a sustainable and efficient approach to enhancing the durability and protective performance of concrete in bridge applications.

Keywords: nanosilica, microorganisms, bacillus pasteurianus, bridge cracks, self-repairing.

Received: 23 April 2025; Accepted: 16 July 2025; Available online: 20.10.2025.

INTRODUCTION

With the acceleration of urbanization, bridges, as critical infrastructures, are subjected to increasing traffic pressure and severe environmental loads. Reinforced concrete structures of bridges inevitably develop cracks during service due to loading, temperature/humidity fluctuations, and chemical attack[1–3]. These cracks provide infiltration channels for corrosive media (e.g., chloride ions, water), accelerating the corrosion of reinforcing steel and reducing the structural bearing capacity. In serious cases, they even cause safety accidents, leading to high maintenance costs and waste of resources. Traditional crack repair methods (such as caulking, surface coating, pressure grouting, etc.) have many limitations. Organic materials are costly and short-lived. Inorganic materials have poor adhesion. Furthermore, these methods are often difficult to make lasting repairs and are prone to secondary damage[4].

Microbial self-repairing technology has received much attention in recent years as an emerging and environmentally friendly concrete repair method[5]. This technique utilizes the metabolic activities of specific microorganisms (e.g., *Bacillus pasteurii*) to convert calcium source material into $CaCO_3$ crystals to fill and repair concrete cracks (CCs)[6, 7]. To overcome the difficulties of a harsh environment and high alkalinity for bacterial growth, Jiang et al.[8] suggested using the microbial-induced carbonate precipitation approach for self-repairing concrete fractures. The results showed that this technique could effectively enhance the self-repairing ability of concrete and improve the repair efficiency. Qian et al.[9] proposed the use of *Bacillus glabrata* as a new mineralization pathway to improve the repair speed and solve the problem of ammonia emission by addressing the problems of hidden cracks and slow repair speed in CC repair. The results showed that *Bacillus coli* performed better in terms of repair speed and environmental adaptability compared to *Bacillus pasteurii*. Zhang et al.[10] suggested designing and mass-producing self-repairing agents with microbial spores and a calcium source in order to solve the issue of CCs self-repairing in ship lock projects. They then tested the agents using the spray-drying method. The findings demonstrated that the parameters of the concrete mix and the growth of the hardened concrete's compressive strength (CS) were not significantly impacted by the inclusion of a self-repairing agent. In practice, CCs were completely healed within 60 days and crack leakage was effectively blocked. However, there is still room for improvement in the efficiency of microbial self-repairing and the mechanical properties of the repair products.

Nanomaterials, especially nanosilica (nano-SiO_2), show great potential in improving concrete properties due to their high specific surface area (SSA), high reactivity, and excellent mechanical properties[11]. Hakeem et al.[12] addressed the optimization of ultra-high-performance concrete properties and investigated the effects of microsteel fibers and nano-SiO_2 on concrete properties. The high temperature and mechanical properties of the mixtures were calculated by adding different contents of micro steel fibers and nano-SiO_2. The results showed that 6% nano-SiO_2 as a replacement of cement was the optimal solution, which increased the CS by 21% compared to 0% nano-SiO_2. To address the issue of performance enhancement of recycled concrete, Yunchao et al.[13] developed modified activated carbon by using silica fume and nano-SiO_2 as composite additives. According to the findings, the composite addition of silica fume and nano-SiO_2 enhanced the synthesis of hydrated calcium silicate and strengthened recycled concrete during both the early and late curing stages. Tawfik et al.[14] assessed the impact of nano-silica oxide and nano-waste ceramics on the characteristics of Portland cement concrete in an attempt to address the sustainable use of building waste. The outcome revealed that the concrete strength reached its maximum value at all curing ages when the nano-waste ceramic content was 6%, but the strength decreased slightly above 10%. Ali et al.[15] investigated the impact of varying nano-SiO_2 levels on the characteristics of concrete in an attempt to solve the issue of forecasting the CS of concrete. Six regression models were also included in the study to examine the connection between CS and the ratio of concrete mix. With a coefficient of determination as high as 0.96 and a root mean square error of only 3.49 MPa, the whole quadratic regression model demonstrated the highest prediction accuracy, according to the results. To increase the performance of recycled aggregate concrete, Liang et al.[16] suggested combining die casting with nano-SiO_2 particles. According to the results, this approach significantly reduced the overall porosity and enhanced the CS of recycled aggregate concrete by 143%. The impact of nano-SiO_2 on the macroscopic characteristics of concrete has been the primary focus of previous research.

In summary, both microbial self-repairing and nanomaterials have made some progress in the field of concrete repair. However, the research on combining the two to improve the repair efficiency and durability still needs to be deepened, especially to optimize the synergistic effect of nano-SiO_2 with *Bacillus pasteurii*. This study aims to develop a novel self-repairing material for bridge CCs by combining nano-SiO_2 with *Bacillus pasteurii* bacterial solution. The effects of nano-SiO_2 on the growth of microorganisms, the mineralization process, and the performance of the repaired concrete are systematically investigated to reveal the synergistic mechanism. This can offer a theoretical foundation and technical assistance for the creation of effective, durable, and eco-friendly bridge crack repair technologies.

METHODS AND MATERIALS

Research material

Nano-modified materials

The nanomaterial used in the study was nano-SiO_2, which was an odorless, non-toxic, and water-insoluble powder. It had the advantages of high purity, good stability, large SSA, and small particle size (PS)[17]. The nano-SiO_2 used in the experiment was sourced from the International Joint Laboratory of Nano-Biotechnology, Ningbo Engineering College, model 570, with a PS of about 25–35 nm.

Microbial strain

The microorganism used in this study was *Bacillus pasteurii*, which was purchased from the American Therapeutic Collection Center (ATCC) under the strain number ATCC 11859. Its cells were rod-shaped, with a length of about 3 μm and a diameter of about 2 μm. The diameter of the budding state was about 0.8 μm, and it was rounded. This strain exhibited high urease activity and was able to grow and produce spores in an alkaline environment. According to the growth curve provided by ATCC and the results of urease activity measurement, the optimal growth temperature of the strain used in this study was 30 °C. The composition of the strain medium used in the experiment included urea, meat extract, and peptone.

Test raw materials

The raw materials used in the test included P.O. 42.5 ordinary silicate cement produced by Tangshan Hongya Cement Co., Ltd, ordinary construction sand with PS ranging from 0.08 to 2.00 mm, crushed stone aggregates with different PS ranges, and tap water.

Other test reagents and equipment

The test reagents are shown in Table 1.

Table 2 displays the test apparatus.

Test method

Bacillus pasteurii medium preparation

The liquid medium was formulated as follows ($g \cdot L^{-1}$): urea 20.0, beef paste 3.0, Bacto peptone 5.0. 0.8 L of ultrapure water (resistivity≥18.2 MΩ-cm, Milli-Q, Millipore, USA) was added to an enameled cup and brought to a boil, then the above reagents were added sequentially and stirred until completely dissolved. The solution was boiled 3 times to ensure complete dissolution. The solution was transferred to a sterilized conical flask, sealed with a sealing film and sterilized in an autoclave (121 °C, 1.2 bar, 20 min).

Cultivation and storage of Bacillus pasteurii

Perform the following operations under sterile conditions: The ultra-clean bench was sterilized using a UV lamp (30 min). The outer surface of the ampoule was wiped with 75% alcohol, and the tip of the ampoule was

Table 1. MOFs prepared from PET waste using the hydrothermal method

Name	Specifications	Manufacturer
Nano-SiO_2	≥ 99.5%	Xuancheng Jingrui New Materials Co., Ltd
Calcium lactate	≥ 98%	Nanjing Songguan Biotechnology Co., Ltd
Sodium alginate	≥ 95%	Shandong Yatu Biotechnology Co., Ltd
Urea	≥ 99%	Dongguang Chemical Co., Ltd
Peptone	BR	Wuhan Jiyesheng Chemical Co., Ltd
Beef extract	BR	Shandong Topu Bioengineering Co., Ltd
Polyvinyl alcohol (PVA, MW: [100,000])	≥ 99%	Shanghai Hujian Laboratory Equipment Co., Ltd
Ethylenediaminetetraacetic acid calcium	≥ 99%	American AAT Bioquest
Ethylenediaminetetraacetic acid calcium indicator	AR	American AAT Bioquest

Table 2. MOFs prepared from PET waste using the solvothermal method

Name	Model	Manufacturer
Constant temperature oscillator	THZ-101	Shanghai Heheng Instrument Equipment Co., Ltd
DHG series heating and drying oven	DHG-9140A	Zhucheng Dingchuan Machinery Co., Ltd
Barnstead	UPW-III	Shenzhen Medtech Biotechnology Co., Ltd
Clean bench	JS-1000	Beijing Jingcheng Chuangxin Intelligent Technology
High speed centrifuge	HC-100K	Zhejiang Sanlian Environmental Protection Technology Co., Ltd
High-pressure steam sterilization pot	YXQ-LS-50	Guangdong Kebao Experimental Equipment Co., Ltd
High resolution field emission scanning electron microscope (FE-SEM)	SEM-8000	Thermo Fisher Scientific, USA
X-ray diffractometer (XRD)	XRD-6000	
Flowability tester	FL-2020	Hebei Dahong Experimental Instrument Co., Ltd
Electric flux meter	EC-100	Shanghai Rongjida Instrument Technology Co., Ltd
RCM chloride ion migration coefficient (CIMC) tester	RCM-2021	Beijing Durable Weiye Technology Co., Ltd
Carbonization box	CC-500	Shanghai Rongjida Instrument Technology Co., Ltd

heated over the flame of an alcohol lamp to break it. A small amount of sterile water was added to dissolve the lyophilized bacterial powder. The dissolved bacterial solution was inoculated into sterilized liquid medium and incubated at 30 °C for 24 h to obtain the initial strain. To create the functioning bacterial solution, the original strain was then injected into a new liquid medium and cultured for 24 hours at 30 °C and 150 rpm. The working bacterial solution was stored in the refrigerator at 5 °C. The initial strain was mixed with 20% ($v \cdot v^{-1}$) glycerol and frozen in –70 °C refrigerator for long-term storage.

Preparation of nano-SiO_2 modified bacterial solution

For nano-SiO_2 modified bacterial solution preparation, PVA and sodium alginate were first needed to be dissolved by adding them to a water bath at 95 °C in a certain ratio and cooled to room temperature. Next, it was fused with a bacterial solution. Subsequently, 11 g of nano-SiO_2 was added and stirred for 15 min. The nano-SiO_2 modified bacterial solution was prepared by adding sodium hydroxide solution at a concentration of 1 $mol \cdot L^{-1}$ to adjust the pH of the mixture to pH =11. A total of five ratios of nano-SiO_2 modified bacterial solution were prepared in the experiment. The details are shown in Table 3.

Preparation of concrete specimens

The concrete mixing ratio ($kg \cdot m^{-3}$) was 432 cement, 558 sand, 1242 gravel, and 168 water. The water/cement ratio ($w \cdot c^{-1}$) was 0.39. Water, sand, cement, and gravel were put into a forced mixer in sequence and mixed for 5 min. Fresh concrete was poured into φ100 mm×100 mm cylindrical molds, and the vibrating table vibrated the concrete for 10–15 s to ensure the compactness. For 28 days, the specimens were cured under conventional curing conditions, which included a temperature of 20 ± 2 °C and a relative humidity of at least 95%.

Preparation of artificial cracks

The surface of the concrete specimens cured for 28 days was wrapped with tape to prevent complete fracture of the specimens during splitting. Until a noticeable crack developed in the middle of the specimen, the specimens were put on a universal testing machine (UTM) with displacement regulated loading at a rate of 0.5 $mm \cdot min^{-1}$. A steel spacer with a thickness of 0.35–0.50 mm was inserted into the crack, and the crack width was controlled to be in the range of 0.35–0.50 mm. To ensure the accuracy of the crack width, a digital vernier caliper with an accuracy of 0.01 mm is used to measure the crack width multiple times, and the average value is taken as the final crack width. At the same time, digital image analysis software is used to process the crack images, further verifying the accuracy of crack width to ensure the reliability of subsequent experimental results. The specific process is shown in Fig. 1.

Table 3. MOFs prepared from PET waste using the mechanochemical method

Slurry ratio	Group A	Group B	Group C	Group D	Group E
Water (mL)	300	300	300	300	300
Sodium alginate (g)	5	11	17	23	29
Nano-SiO_2 (g)	11	11	11	11	11
Polyvinyl alcohol (g)	5	5	5	5	5
Bacteral solution (mL)	300	300	300	300	300

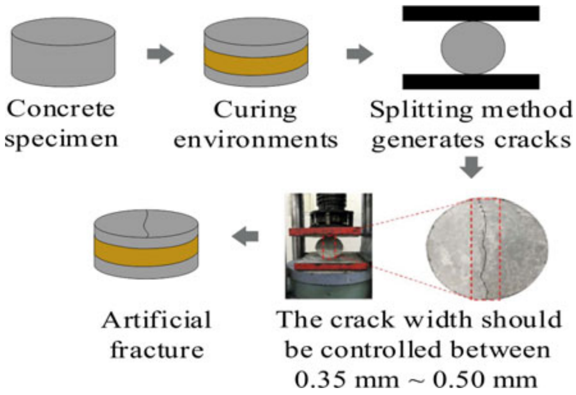

Figure 1. Preparation process of artificial cracks

Crack repair process

Dust and loose particles were removed from the crack surface with a brush and blown dry with compressed air. The prepared nano-SiO_2 modified bacterial solution (Group A) was uniformly applied to the surface of the cracks (the amount of application was about 0.5 mL · cm^{-2}). To ensure the uniformity of coating thickness, a coating thickness gauge with an accuracy of 0.01 mm was used to predict the surface of the specimen and record the initial thickness before applying the nano SiO_2 modified bacterial solution. After applying the solution, use the coating thickness gauge again to measure multiple times at different positions on the surface of the specimen, record the coating thickness data, and calculate the average value. Control the coating thickness within the range of 0.2 mm ± 0.02 mm. Subsequently, 5% (w · v^{-1}) calcium lactate solution was evenly sprayed onto the crack surface with a spray bottle and left for 15 min. The above steps were repeated three times. The repaired specimens were further cured under standard curing conditions for 3 days. The procedure is shown in Fig. 2.

Performance testing

Mobility testing: The flowability of the bacterial solution in different ratios was determined using a flow meter (according to GB/T 2419-2005).

Mineralization performance testing: The mineralization efficiency (ME) of bacterial solution was determined by ethylenediamine tetraacetic acid (EDTA) titration. 200 mL of bacterial solution was taken, and 0.05 mol · L^{-1} of EDTA and calcium indicator were added. A 0.1 mol · L^{-1} NaOH solution was added to the solution to titrate it until its burgundy hue turned blue. The Ca^{2+} concentration was calculated from the EDTA consumption, and then the ME was calculated.

Sediment morphology analysis: The precipitates from the bacterial solution were analyzed by FE-SEM (accelerating voltage: 10 kV) and energy dispersive spectrometer (EDS) for morphological observation and elemental analysis. The precipitates were analyzed by XRD (Cu Kα radiation, scanning range: 10–80°, scanning speed: 4° · min^{-1}).

Chloride migration coefficient (CMC) test: CMCs of concrete specimens were determined according to the RCM method (NT Build 492). CMCs of untreated specimens (blank group), specimens treated with water only (pure water group), and specimens treated with nano-SiO_2 modified bacterial solution (bacterial solution group) were tested.

Electrical flux test: The electrical flux of concrete specimens of different treatment groups was determined using an electrical flux tester (6 V constant voltage, 6 h test time).

Carbonation depth test: Concrete specimens from different treatment groups were placed in a carbonation chamber (CO_2 concentration: 20 ± 3%, temperature: 20 ± 2 °C, relative humidity: 70 ± 5%). The specimens were removed on days 3, 7, 10, 13, and 15. The depth of carbonization was measured by spraying 1% phenolphthalein indicator on fresh sections after splitting.

Multiple fix performance testing: Crack images were taken vertically using a high magnification camera (model: D780, Nikon, Japa) before the repair, after the first repair, and after the second crack repair. To determine the quantity of pixels in the cracked area (CA), the images were binarized using the Otsu thresholding method after being imported into ImageJ software. Area repair rate = (quantity of pixels of repaired CA/quantity of pixels of initial CA) × 100%. The secondary cracks were generated in the same way as the initial cracks.

RESULTS AND DISCUSSION

Flowability of Nano-SiO_2 modified bacterial solution

Figure 3 displays the outcomes of flowability experiments for bacterial solutions with varying sodium alginate

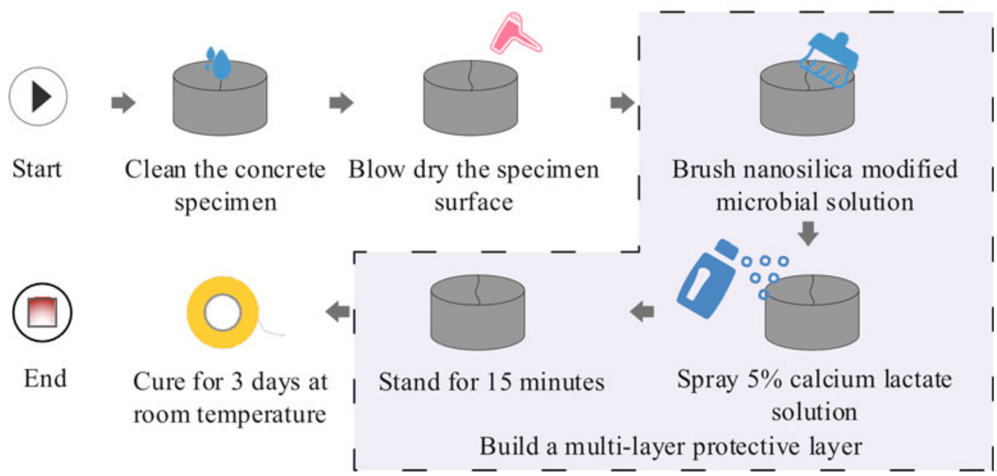

Figure 2. Crack repair process flow

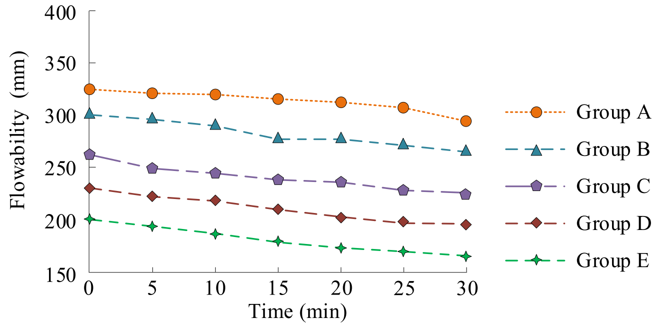

Figure 3. Liquidity test results with different mix proportions

levels. The bacterial solution's mobility dramatically dropped as the sodium alginate level rose. At the beginning of the test (0 min), the flowability of the bacterial solution in group A was 325 mm, while that in group E was only 200 mm. The flowability of the bacterial solution decreased in all groups with time. This could be attributed to the gelling effect of PVA and sodium alginate[18]. Considering the requirement of flowability (>300 mm) for subsequent remediation processes and the possibility that too much sodium alginate may affect the microbial activity[19], group A ration (5 g sodium alginate) was finally selected for subsequent experiments.

Effect of pH on microbial growth and ME

Figure 4 displays the growth curves and ME of bacteria at various pH levels. In Fig. 4a, the growth of microorganisms went through four typical phases: retardation, logarithmic growth, stabilization, and decay. Among them, the higher the pH value, the lower the optical density of the bacterial solution, and the lower the concentration of the bacterial solution. However, when the pH value was too high, the growth of microorganisms occurred abnormally. Therefore, the pH value used for the study was 11. In Fig. 4b, the ME curve of the bacterial solution had the same trend as the growth curve of microorganisms, but with some lag. At pH = 11, the optical density of the bacterial solution was the highest at 32 h (OD_{600} = 3.84). However, the ME reached its maximum value only at 36 h, with a value of 2.18 mol · h^{-1}. After 36 h, the ME of the bacterial solution gradually decreased. Taken together, the tested bacterial solution could not exceed 36 h. The above results showed that *Bacillus pasteurii* had better growth and mineralization ability in alkaline environment, which was compatible with its application in CC repair.

Morphology and compositional analysis of nano-SiO_2 modified bacterial solution precipitates

XRD analysis

Figure 5 displays the XRD spectra of the mineralization products caused by various calcium sources. The precipitates induced by the two calcium sources (calcium lactate and calcium acetate) were calcite-type $CaCO_3$. The main diffraction peaks (2θ = 19°, 24°, 32°, 34°, 39°, 43°, 44°, 53°, 57°) were in agreement with those of a standard calcite card (JCPDS No. 05-0568). It was difficult to determine the optimal calcium source and further analysis was needed.

SEM and EDS analysis

SEM images of $CaCO_3$ crystals synthesized with different calcium sources are shown in Fig. 6. In Fig. 6a, the surface of $CaCO_3$ crystals synthesized using calcium

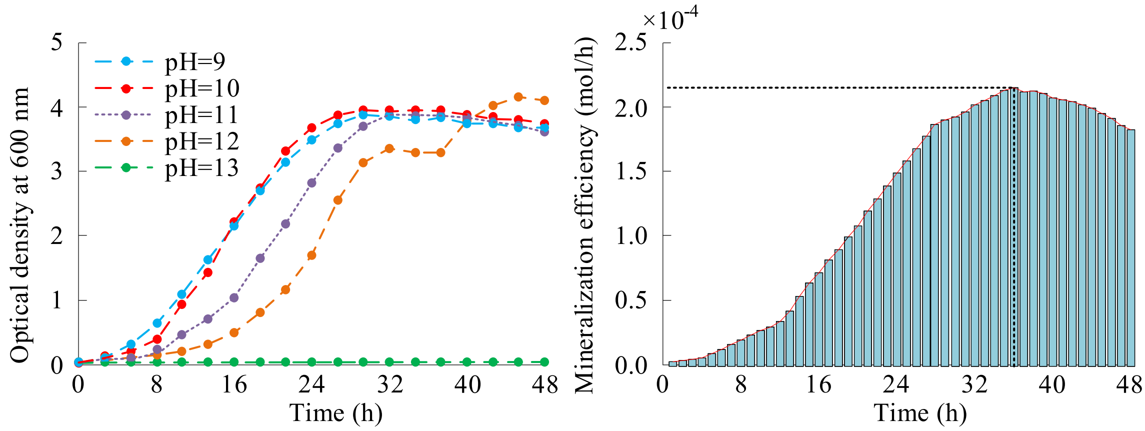

Figure 4. The growth of microorganisms and the ME of bacterial solution: (a) microbial growth curve and (b) ME

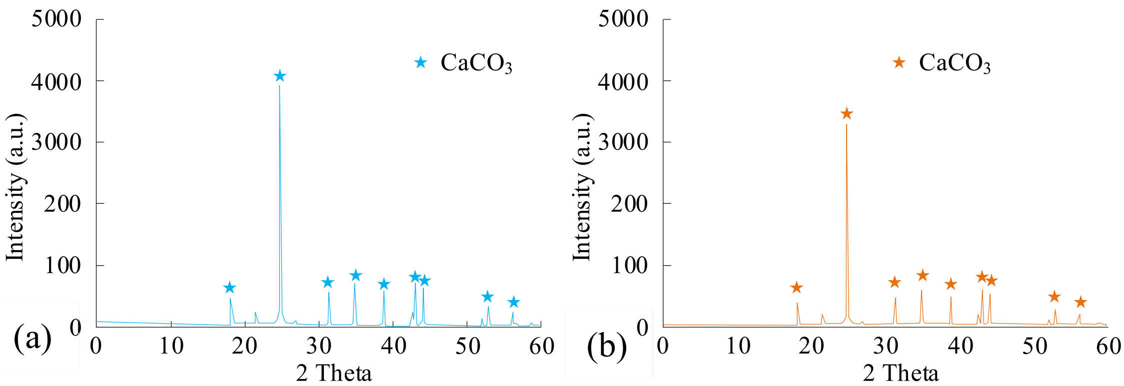

Figure 5. XRD analysis results of mineralization reactions induced by different calcium sources: (a) XRD pattern of calcium acetate as calcium source and (b) XRD pattern of calcium lactate as calcium source

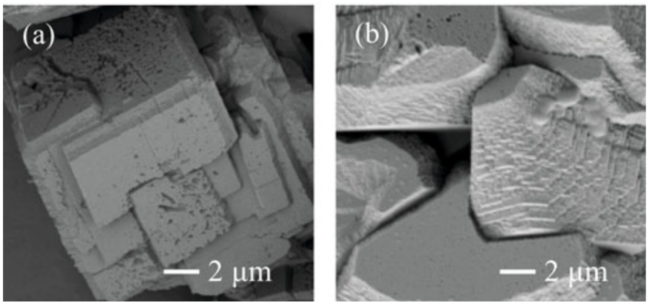

Figure 6. SEM images of $CaCO_3$ crystals synthesized by different calcium sources: (a) calcium acetate and (b) calcium lactate

acetate as the calcium source was smoother, and no obvious grooves existed. In Fig. 6b, the surface of $CaCO_3$ crystals synthesized using calcium lactate as the calcium source was rougher, with obvious grooves.

The EDS spectra of $CaCO_3$ crystals synthesized by different calcium sources are shown in Fig. 7, along with the proportions of individual atoms. In Figs. 7a and b, the crystals induced by different calcium sources contain C, O, and Ca atoms, but with different proportions. In Fig. 7c, the percentage of calcium atoms in the $CaCO_3$ crystals induced by calcium lactate was 17.68%. In contrast, the proportion of calcium atoms in calcium acetate was as high as 27.82%, which was much higher than that of calcium lactate. This meant that calcium lactate adsorbed Ca^{2+} more efficiently and synthesized crystals more efficiently. The reason is that the surface of calcium carbonate crystals induced by calcium lactate is rougher, with obvious grooves, making the crystals have a higher specific surface area and more adsorption sites, resulting in stronger adsorption capacity. At the same time, ion adsorption kinetics experiments showed that the adsorption amount of Ca^{2+} by calcium lactate solution was significantly higher than that of calcium acetate solution in the same time, and the adsorption rate was faster. This indicates that calcium lactate has higher efficiency in adsorbing Ca^{2+} and can more effectively promote the precipitation of calcium carbonate. Therefore, the optimal calcium source was calcium lactate.

Concrete performance testing

CMC

The study looked into how concrete specimen performance was affected by varying coating intervals and coat counts. In Fig. 8a, the CMC decreases with the quantity of coating times. Among them, the CIMC of the bacterial solution group decreased to about 8.67×10^{-13} $m^2 \cdot s^{-1}$ after 3 times of application. The migration coefficients of chloride ions in the blank group and the pure water group were as high as 23.13×10^{-13} $m^2 \cdot s^{-1}$ and 16.47×10^{-13} $m^2 \cdot s^{-1}$, respectively, which were significantly higher than those in the bacterial solution group. This indicated that the nano-SiO_2 modified bacterial solution formed a dense protective layer on the concrete surface and effectively prevented the penetration of chloride ions. When the number of coats was increased again, the CMC did not change much, which meant that the number of coats had reached saturation. Considering that too many coats may lead to the problem of peeling, the number of coats was set to 3. In Fig. 8b, the painting time interval also affects the CIMC. When the painting time interval was 15 min, the CMC of the bacterial solution group was lower than that of pure water group, which was 8.48×10^{-13} $m^2 \cdot s^{-1}$ and 16.37×10^{-13} $m^2 \cdot s^{-1}$, respectively. When the interval time was increased again, the CMC did not change much. Therefore, the painting time interval should be set to about 15 min.

Electrical flux and carbonation depth

The study continued to explore the electrical flux as well as the depth of carbonation of different groups of concrete specimens. Figure 9 displays the findings. In this regard, the electrical flux was a measure of chloride ion migration in concrete, and a lower electrical flux represents a lower chloride ion permeability of concrete, implying a higher capacity for repair and protection.

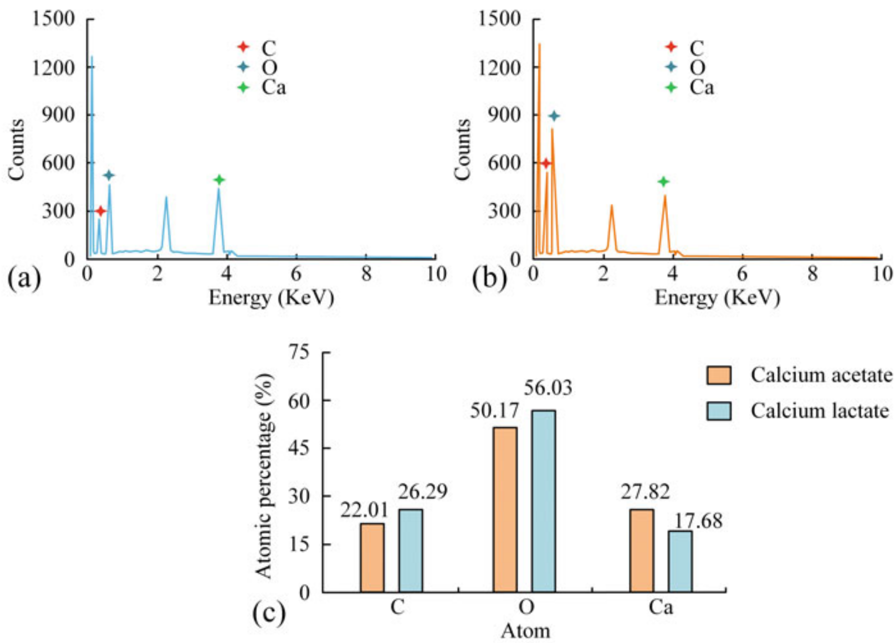

Figure 7. EDS spectrum of $CaCO_3$ crystal and the ratio of each atom: (a) energy spectrum of calcium acetate, (b) energy spectrum of calcium lactate, and (c) atomic ratio of calcium carbonate crystals

The electrical flux of the bacterial solution group in Fig. 9a was 327 ºC, which was much lower than that of the blank and pure water groups. It indicated that the nano-SiO_2 modified bacterial solution treatment significantly improved the resistance of concrete to chloride ion penetration, with the best self-repairing effect. In Fig. 9b, the carbonization depth of the bacterial solution group was always significantly lower than that of the blank and pure water groups during the 15-day carbonization test. On the 13th day, the carbonation depth of the bacterial solution group was only 2.8 mm, while that of the water-pure group was as high as 6.57 mm, and that of the blank group was as high as 7.82 mm. This indicated that the $CaCO_3$ precipitation generated by the nano-SiO_2 modified bacterial solution effectively filled the pores and microcracks on the concrete surface. It prevented the intrusion of CO_2 and thus slowed down the carbonation process.

Multiple repair performance

The repair effects of the bacterial solution group on the first and second cracks are shown in Fig. 10. Figures 10a and b revealed that the repair effect of nano-SiO_2 modified bacterial solution was superior in both first and second crack repair. In Fig. 10c, after 28 days of repair, the area repair rate of nano-SiO_2 modified bacterial solution was more than 95% in both the first and second crack repair. It indicated that the nano-SiO_2 modified bacterial solution had excellent multiple repair capability.

Discussion

Nano-SiO_2 has high SSA and porosity, which can provide more attachment surfaces and nutrient exchange sites for microorganisms, and thus promote the growth of microorganisms. Meanwhile, nano-SiO_2 can change the metabolic pathway of microorganisms. In the process of microbial-induced $CaCO_3$ precipitation, nano-SiO_2 mainly affects the $CaCO_3$ precipitation process by changing the charge distribution on the bacterial surface and providing nucleation sites. In the experiment, the surface of nano-SiO_2 was used to adsorb the generated Ca^{2+} ions and react with carbon dioxide to generate $CaCO_3$, which promoted the mineralization reaction. The synergistic effect of nano-SiO_2 and microorganisms was the most critical mechanism in microbial self-repairing concrete. Specifically, when microorganisms colonized the crack surface, nano-SiO_2 promoted their growth and metabolism by providing an attachment platform for microorganisms to accelerate $CaCO_3$ generation. The generated $CaCO_3$ would be deposited at the cracks to fill the micro-cracks and form a protective layer.

The study focused on the effectiveness of incorporating nano-SiO_2 into bacterial solution for the repair of bridge CCs. The test outcomes revealed that the growth of microorganisms at pH 11 showed a similar trend to the ME of the bacterial solution. Therefore, the bacterial solution for conducting the test could not be more than 36 h. The surface of $CaCO_3$ crystals made using calcium lactate as the calcium source was significantly rougher, according to a comparison of the impacts of two distinct calcium sources on the microbial products. Moreover, the percentage of calcium atoms was only

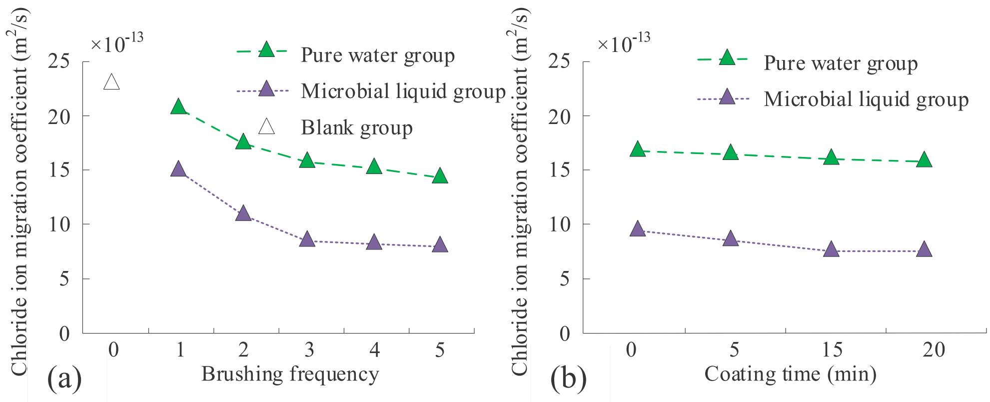

Figure 8. The influence of different painting times and painting time intervals on the performance of specimens: (a) the influence of brushing frequency on the chloride ion migration coefficient and (b) the influence of coating time on the migration coefficient of chloride ions

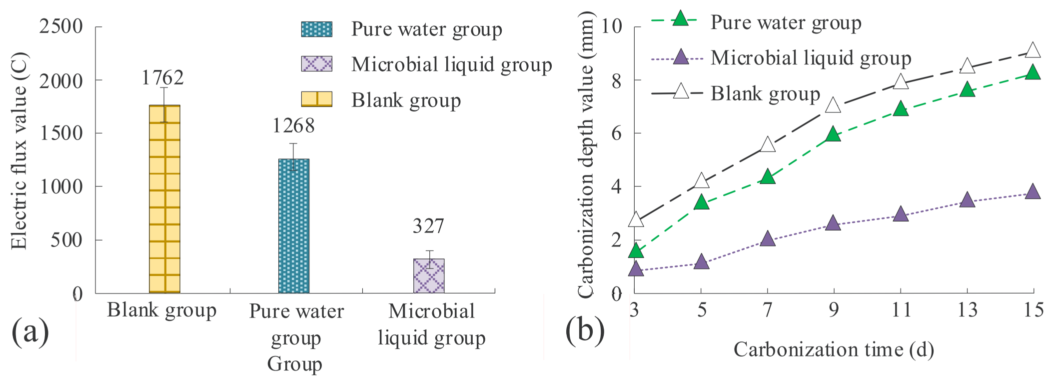

Figure 9. Electric flux and carbonation depth of concrete test blocks in different groups: (a) electric flux values of different groups and (b) carbonization depth values of different groups

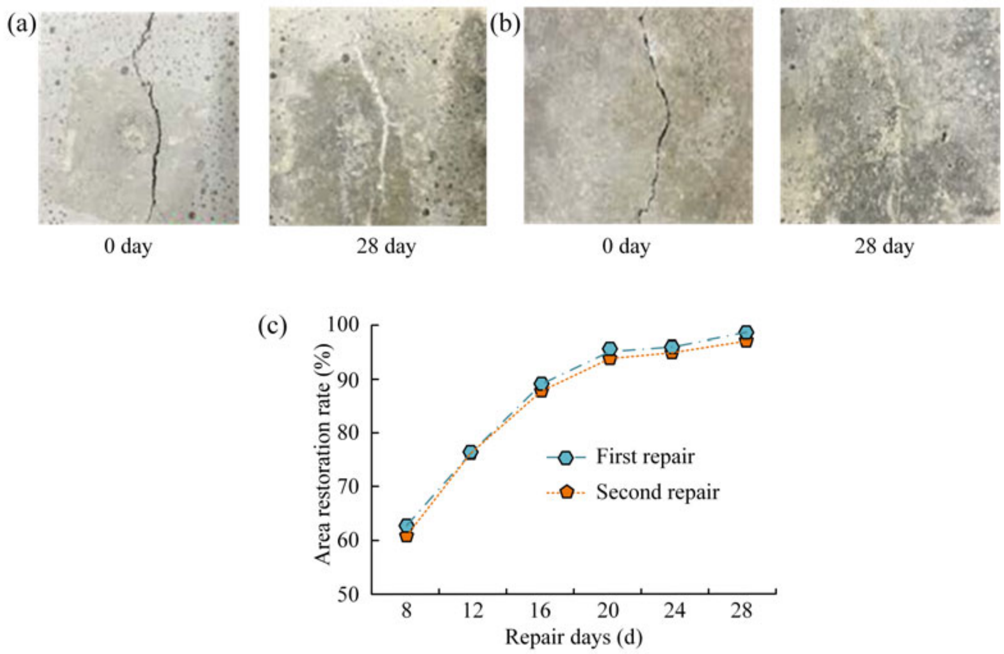

Figure 10. Multiple repair performance of bacterial solution group: (a) before and after the first crack repair, (b) before and after the second crack repair, and (c) area restoration after 28 days

17.68%, which was lower than that of calcium acetate. It was shown that calcium lactate adsorbs Ca^{2+} ions more efficiently and reacts with carbon dioxide to produce more $CaCO_3$, improving the ME. Similarly, Jiang et al.[20] suggested using microbially generated carbonate precipitation to increase concrete's capacity for self-repairing. The results showed that the selection of both the appropriate sequence of nutrient addition and the carrier could effectively promote the growth and mineralization reaction of bacteria, thus enhancing the crack repair effect. Both emphasized the importance of microbial growth and ME on the effectiveness of crack repair. However, the advantage of this study was to explore the effect of nano-SiO_2 incorporation into the bacterial solution on the ME and further optimize the carbonate precipitation process.

Compared with the blank group and the pure water group, the CIMC of the bacterial solution group used in the study was only about 8.67×10^{-13} $m^2 \cdot s^{-1}$ after three times of bacterial solution application. Meanwhile, the CIMC was only 8.48×10^{-13} $m^2 \cdot s^{-1}$ at the coating time interval of 15 min. It indicated that the incorporation of nano-SiO_2 into the bacterial solution improved the impermeability of concrete self-repair. Existing studies indicated that microbial self-repairing concrete was relatively weak in preventing chloride ion migration[8]. However, the study effectively enhanced the mineralization ability of microorganisms and the repair effect of cracks by introducing nano-SiO_2, and the CIMC was lower compared with the values in other studies, indicating that this method had obvious advantages in enhancing the impermeability of concrete. In addition, this process could greatly improve the efficiency of crack repair. After secondary cracking, the cracks could still be effectively repaired, and a protective layer could be formed. Meanwhile, the deposition rate of $CaCO_3$, a mineralization product of microorganisms, was improved by the addition of nano-SiO_2, and the effect of repair was more durable. To address the problem of CCing, Sivamani et al.[21] proposed a new technique of bacterial self-repairing through microbial-induced calcite precipitation. The effect of *Bacillus subtilis* and *Escherichia coli* on the properties of concrete was investigated. The outcomes revealed that the CS of the concrete containing bacteria increased by a maximum of 12.8% compared to the control concrete. SEM analysis showed that calcite precipitation effectively closed the surface cracks and improved the performance of concrete. The similarity between the two studies was that both utilized microbial-induced calcite precipitation to achieve CC repair. The distinction was that the study added nano-SiO_2 to the bacterial solution, which increased the microbial mineralization reaction's efficiency and the concrete's capacity for self-healing.

CONCLUSION

In this study, the application of nano-SiO_2 modified bacterial solution in bridge CC repair was systematically investigated, and the following main conclusions were obtained:

1. The bacterial solution ratios are optimized: At a sodium alginate content of 5 g (Group A), the bacterial solution had a suitable flowability for construction applications.

2. The optimal restoration process was determined: The bacterial solution was applied 3 times at an interval of 15 min, which significantly reduced the CMC of the concrete (up to 8.48×10^{-13} $m^2 \cdot s^{-1}$) and improved the impermeability.

3. The restoration was confirmed: The nano-SiO_2 modified bacterial solution treatment significantly reduced the electrical flux (327 °C) and the carbonation depth (2.8 mm after 13 days) of the concrete compared to the blank and pure water groups.

4. Multiple repair capability was verified: After 28 days of repair, the area repair rate of the first crack repair was 96.83% ± 1.82%, and the area repair rate of the second crack repair was 95.52% ± 1.51%. There

was no statistical difference between the two ($p>0.05$). Compared with other existing repair methods, the repair rate of this study has significant advantages. Among them, the repair rate reported in the research of scholars such as Wang is around 90%, which is lower than 95%[22].

5. The mechanism of action was elucidated: nano-SiO_2 promoted microbial attachment by providing a larger SSA, modulated $CaCO_3$ crystal growth, and synergized with PVA and sodium alginate to improve remediation efficiency and durability.

In summary, nano-SiO_2 modified bacterial solution is a promising self-repairing material for bridge CCs, which can significantly improve the durability and service life of concrete structures. However, this study is mainly based on laboratory conditions. Future research should focus on field tests to further verify its long-term performance and practical application effects, and to evaluate the cost of the repair material.

LITERATURE CITED

1. Zhu, J., Shen, D., Xie, J., Jin, B. & Wu, S. (2022). Transformation mechanism of carbamic acid elimination and hydrolysis reaction in microbial self-healing concrete. *Molecular Simulation*. 48(8), 719–735. DOI: 10.1080/08927022.2022.2049773.

2. Xu, J., Wang, X., Yao, W., Kulminskaya, A.A. & Shah, S.P. (2024). Microbial-inspired self-healing of concrete cracks by sodium silicate-coated recycled concrete aggregates served as bacterial carrier. Frontiers of Structural and Civil Engineering. 18(1), 14–29. DOI: 10.1007/s11709-023-0993-7.

3. Njau, M. W., Mwero, J., Abiero-Gariy, Z. & Matiru, V. (2022). Effect of temperature on the self-healing efficiency of bacteria and on that of fly ash in concrete. *Internat. J. Engin. Trends Technol.* 70(4), 174–187. DOI: 10.14445/22315381/IJETT-V70I4P215.

4. Ali, M. F., Mukhtar, H. & Dufosse, L. (2023). Microbial calcite induction: A magic that fortifies and heals concrete. Internat. *J. Environ. Sci. Technol*. 20(1), 1113–1134. DOI: 10.1007/s13762-022-03941-2.

5. Yun, L. (2024). Investigation of crack healing and optimization of microbe carrier for microbial self-healing of concrete crack. Journal of The Korea Institute for Structural Maintenance and Inspection. 28(4), 62–67. DOI: 10.11112/jksmi.2024.28.4.62.

6. Abu el-Hassan, K., Hakeem, I.Y.Y., Amin, M., Tayeh, B.A.A., Zeyad, A.M.M., Agwa, I.S. & Elsakhawy, Y. (2024). Effects of nano titanium and nano silica on high-strength concrete properties incorporating heavyweight aggregate. *Structural Concrete*. 25(1), 239–264. DOI: 10.1002/suco.202300232.

7. Shim, S., Kim, J., Cho, G.C. & Lee, S.W. (2023). Stereo-vision-based 3d concrete crack detection using adversarial learning with balanced ensemble discriminator networks. Struct. Health Monitoring-an Internat. J. 22(2), 1353–1375. DOI: 10.1177/14759217221097868.

8. Jiang, L., Li, P., Wang, W., Zhang, Y. & Li, Z. (2024). A self-healing method for concrete cracks based on microbial-induced carbonate precipitation: Bacteria, immobilization, characterization, and application. *J. Sust. Cement-Based Mat*. 13(2), 222–242. DOI: 10.1080/21650373.2023.2263447.

9. Qian, C., Zheng, T. & Rui, Y. (2021). Living concrete with self-healing function on cracks attributed to inclusion of microorganisms: Theory, technology and engineering applications—a review. *Sci. China Technol. Sci.* 64(10), 2067–2083. DOI: 10.1007/s11431-021-1879-6.

10. Zhang, X. & Qian, C. (2022). Engineering application of microbial self-healing concrete in lock channel wall. *Marine Geores. & Geotechnol*. 40(1), 96–103. DOI: 10.1080/1064119X.2021.1871690.

11. Garg, R., Garg, R. & Eddy, N.O. (2023). Microbial induced calcite precipitation for self-healing of concrete: A review. *J. Sust. Cement-Based Mat.* 12(3), 317–330. DOI: 10.1080/21650373.2022.2054477.

12. Hakeem, I.Y., Amin, M., Abdelsalam, B.A., Tayeh, B.A., Althoey, F. & Agwa, I.S. (2022). Effects of nano-silica and micro-steel fiber on the engineering properties of ultra-high performance concrete. *Struct. Engin. Mech.* 82(3), 295–312. DOI: 10.12989/sem.2022.82.3.295.

13. Yunchao, T., Zheng, C., Wanhui, F., Yumei, N., Cong, L. & Jieming, C. (2021). Combined effects of nano-silica and silica fume on the mechanical behavior of recycled aggregate concrete. *Nanotechnol. Reviews.* 10(1), 819–838. DOI: 10.1515/ntrev-2021-0058.

14. Tawfik, T.A., Metwally, K.A., El-Beshlawy, S., Al Saffar, D.M., Tayeh, B.A. & Hassan, H.S. (2021). Exploitation of the nanowaste ceramic incorporated with nano silica to improve concrete properties. *J. King Saud Univ. Engin. Sci*. 33(8), 581–588. DOI: 10.1016/j.jksues.2020.06.007.

15. Ali, R., Muayad, M., Mohammed, A.S. & Asteris, P.G. (2023). Analysis and prediction of the effect of nanosilica on the compressive strength of concrete with different mix proportions and specimen sizes using various numerical approaches. *Struct. Conc*. 24(3), 4161–4184. DOI: 10.1002/suco.202200718.

16. Liang, Z., Hu, Z., Zhou, Y., Wu, Y., Zhou, X., Hu, B. & Guo, M. (2022). Improving recycled aggregate concrete by compression casting and nano-silica. *Nanotechnol. Rev*. 11(1), 1273–1290. DOI: 10.1515/ntrev-2022-0065.

17. Kannan, G. & Sujatha, E.R. (2022). A review on the choice of nano-silica as soil stabilizer. *Silicon.* 14(12), 6477–6492. DOI: 10.1007/s12633-021-01455-z.

18. Casalino, G., D'Amico, F., Bozzo, G., Dinardo, F.R., Schiavitto, M., Galante, D., Aceti, A., Ceci, E., Romito, D., D'Onghia, F.P., Dimuccio, M.M., Camarda, A. & Circella, E. (2024). In field evaluation of impact on clinical signs of an inactivated autogenous vaccine against *Pasteurella multocida* in rabbits. International *J. Vet. Sci. Med.* 12(1), 39–47. DOI: 10.1080/23144599.2024.2348900.

19. Ahmed Ibrahim Ali, O., Ibrahim Hassanin Mohamed, A., Ibrahim, W., Osama Abd-Al Ftah, R., R Hamed, S. & Fakhry M Abd-Elnaby, S. (2024). Enhancing concrete performance through microbial intervention: A comprehensive experimental study. *Engin. Res. J.* 183(4), 85–106. DOI: 10.21608/erj.2024.311680.1087.

20. Hui, R., Yuting, C., Dee, L., Yang, F. & Jianyun, W. (2022). Microbial-sodium alginate based external repair materials and their synergistic effect on crack repair. J. Chin. Ceramic Soc. 50(8), 2087–2095. DOI: 10.14062/j.issn.0454-5648.20210855.

21. Sivamani, J. (2023). Bio-remediation of cracks – a novel technique to self-heal cracks in the concrete. Europ. J. Environ. Civil Engin. 27(14), 4086–4100. DOI: 10.1080/19648189.2023.2171140.

22. Wang, J., Zhu, J., Li, Y., Zhang, S. & Feng, C. (2025). Evaluation and optimal width ratio selection of microbial mineralization technique in the repair of lining cracks in Xinjiang desert open channel. Scien. Reports. 15(1), 1–16. DOI: 10.1038/s41598-025-01582-2.